

Cross-layer Rate and Power Adaptation Strategies for IR-HARQ Systems over Fading Channels with Memory: A SMDP-based Approach

Ashok K. Karmokar, Dejan V. Djonin and Vijay K. Bhargava, *Fellow, IEEE*

Abstract—Incremental-redundancy hybrid automatic repeat-request (IR-HARQ) schemes are proposed in several wireless standards for increased throughput-efficiency and greater reliability. We investigate transmit power and modulation order adaptation strategies for the IR-HARQ schemes over correlated Rayleigh fading channels using semi-Markov decision process-based model. In order to jointly analyze physical layer and link layer, transmitter model incorporates a finite-size buffer that receives randomly varying traffic from a higher layer application. It is assumed that channel variations can be modeled with a first-order Markov chain. We show that the optimal transmission power and rate adaptation laws under buffering delay and packet overflow constraints can be obtained using the framework of semi-Markov decision process. We discuss three different adaptation models for the IR-HARQ schemes and compare their performances with the non-adaptive scheme. It is shown that unique optimal policy exists for each case and it can be computed using linear programming approach. This optimal policy is then applied for realistic channel fading and incoming traffic samples to evaluate its performance for both hard-decision and soft-decision decoding. Simulation results in general point out that substantial power savings can be achieved using adaptation and also if the transmission-delay requirements are relaxed.

Index Terms—Packet scheduling, cross-layer transmission rate and power adaptation, Incremental redundancy type-II hybrid automatic repeat request system, Correlated fading channel, Semi-Markov decision process, Latency and packet overflow considerations, Rate-compatible punctured convolutional code.

I. INTRODUCTION

Incremental redundancy hybrid automatic repeat request (IR-HARQ) is provisioned as a part of EDGE standard and is also proposed as a part of 3G evolution cellular system standards, such as W-CDMA high speed downlink packet access (HSDPA) and CDMA2000 1x Evolution-Data Optimized (EVDO) for high speed reliable packet data communications [1], [2]. IR-HARQ employs forward error correction (FEC) technique in the physical layer as well as ARQ technique

in the data link layer to cope with the time-varying fading channels, and to guarantee both the high reliability and the high throughput. In IR-HARQ schemes, information packets are first transmitted with no or few parity bits for error detection and correction. Incremental redundancy bits are transmitted upon retransmission request. The receiver combines the transmitted and retransmitted bits together to form a more powerful error correction code to recover the information. Rate compatible punctured convolutional (RCPC) codes proposed in [3] are particularly useful for IR-HARQ systems. RCPC codes are constructed from a single rate $1/N$ convolutional code, wherein a family of higher rate codes is formulated by puncturing successively greater numbers of code symbols. These codes have practical utility in that the system requires a single rate $1/N$ convolutional encoder and a Viterbi decoder [4]. In [3], a truncated IR-HARQ scheme with RCPC is analyzed for transmission over both AWGN channel and ideally interleaved Rayleigh fading channel, assuming independent decoding attempts. The authors of [4] have presented the encoding as well as Viterbi and sequential decoding of high-rate punctured convolutional codes.

Packet errors occur in wireless channels due to various propagation impairments, such as multi-path fading and these errors are correlated in nature [5]. To deal with correlated errors, a first order Markov model with a finite number of states is considered in [6]. The case with only two states dates back to the early work by Gilbert and Elliot [7], [8]. This first order Markov model is widely used for packet communications due to combination of its analytical tractability and accuracy. Generalized type-II HARQ using RCPC which combines the IR-HARQ strategy of Hagenauer with the code-combining ARQ strategy of Chase is analyzed in [9]. In [10], an IR-HARQ with selective combining is investigated over a finite state Markov channel (FSMC) model. Using Markov error structure, throughput estimation methods for adaptive modulation systems combined with ARQ schemes are presented in [5]. In [11], a type-II HARQ system with a finite size receiver buffer is analyzed over a two-state Markov channel using rate $1/2$ convolutional code and truncated HARQ. Adaptive transmissions are powerful techniques to compensate for channel variations. In [12], throughput maximization is analyzed with finite number of power levels and code rates. Performance evaluation for schemes with HARQ and rate adaptation is given in [13]. Coding rate adaptation for type-I HARQ system over a partially observable correlated Rayleigh

Paper approved by R. Fantacci, the Editor for Wireless Networks and Systems of the IEEE Communications Society. Manuscript received February 21, 2006; revised December 6, 2006 and August 27, 2007; accepted November 19, 2007. This work is supported jointly by the Natural Sciences and Engineering Research Council (NSERC) of Canada under a strategic project grant, UBC Graduate Fellowship, and NSERC Postdoctoral Fellowship. The material in this paper was presented in part at the IEEE International Conference on Communications (ICC2006), June 11-15, 2006, Istanbul, Turkey.

The authors are with the Department of Electrical and Computer Engineering, 2332 Main Mall, University of British Columbia, Vancouver, BC, V6T 1Z4, Canada, (e-mail: {ashokk, ddjonin, vijayb}@ece.ubc.ca).

Digital Object Identifier 10.1109/TCOMM.2008.xxxxxx

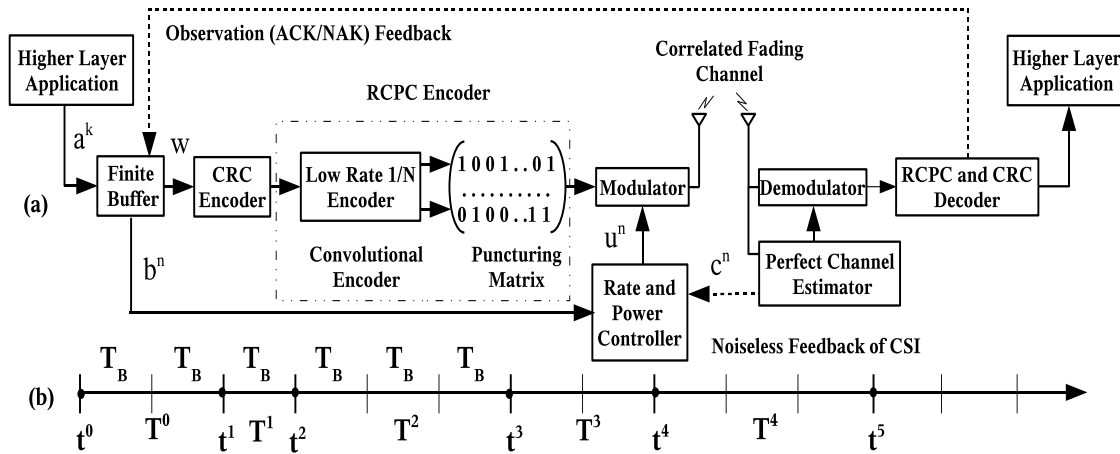


Fig. 1. (a) System diagram of the incremental redundancy hybrid ARQ system and (b) Typical sample path for a SMDP.

fading channel has been studied in [14]. In [15], delay-bounded minimal power transmissions of bursty sources over AWGN and fading channels are studied.

We adapt the transmission power and modulation order of an IR-HARQ system based on both the channel state and the buffer state to minimize three goals: transmission power, buffer delay and packet overflow. Due to incorporation of finite buffer, calculation of delay and overflow is dynamic in nature and we cannot resort to a static optimization problem to find the optimal control policy. Three mentioned objectives are conflicting and therefore the ensuing problem can be formalized as the minimization of average transmission power under the constraints on the average buffering delay and the average packet overflow. Furthermore, we assume that control actions in the IR-HARQ problem are made at the beginning of the transmission and kept unchanged during the possible retransmissions. This assumption is introduced to simplify the optimization and policy implementation setting as discussed in Section III.

Since the optimization criteria is dynamic in nature, the problem falls under the purview of *stochastic dynamic programming* methods [16]. Further, due to stochastic nature of the duration of successive decision-epochs and dependence of the costs on the decision-epoch duration, the optimization problem is formulated as a semi-Markov decision process (SMDP) problem. The optimal solution of the formulated cross-layer adaptation problem is found by converting it into an equivalent auxiliary discrete-time Markov decision process (DT-MDP) problem and utilizing linear programming (LP) methods. To our best knowledge, this is the first work that analyzes SMDP-based cross-layer adaptation law under latency and overflow constraints for IR-HARQ systems.¹ However, SMDP-based framework has been applied in several other network problems previously. In [17], the optimal admission policies for integrated voice/data traffic in CDMA packet radio networks have been derived. A SMDP is used to model the system operation and value iteration algorithm is used to derive the optimal admission policies. Path optimization

problem for inter-switch handoffs is formulated as a SMDP in [18] with the objective of minimizing handoff delay. In [19], a cross-layer optimal admission control policy that tradeoff blocking probability and delay for multiclass CDMA networks is proposed based on a SMDP formulation.

A. Summary of Contributions

We briefly summarize the contributions of this paper below:

- we explore the applicability of the SMDP-based policy optimization for an adaptive IR-HARQ transmission scheme with the objectives of minimizing transmission power, buffering delay, and packet overflow
- we propose a general framework for making scheduling decisions of the rate and power considering cross-layer optimization goals
- we propose and analyze different ways of calculating the costs for different transmission parameters. We also show how to translate the SMDP framework into an MDP framework in order to calculate the optimal policy efficiently. We apply analytically computed optimal policy for realistic channel fading and incoming traffic scenarios to evaluate its performance for both hard-decision and soft-decision decoding.
- the proposed framework can be applied to any system that uses hybrid ARQ method utilizing either incremental-redundancy or packet-combining techniques at the receiver. For example, HSDPA system uses either incremental-redundancy (IR) or Chase-combining techniques. The proposed rate and power adaptation scheme can directly be applied to it for improved performance. Our control framework is of importance for forward link CDMA2000 1xEVDO system that uses IR to enhance the throughput. The only change that should be undertaken is the calculation of packet error rates for different channel states and after different time-slot repetitions [20].

The remaining part of the paper is organized as follows. In Section II, we describe the system model including incoming traffic, buffer and channel models used in the paper. The observation probability for the scheme being considered is also described for both the hard-decision and soft-decision

¹The methodology described in this paper can equally be applied to any HARQ scheme with packet (e.g. Chase) combining at the receiver.

decodings. We explain the formulation of the problem as SMDP and three adaptation models in Section III. In Section IV, the CMDP formulation of the equivalent DT-MDP and its solution techniques are given. The non-increasing and convexity properties of the average power with respect to average delay and overflow constraints are also discussed in this section. We give simulation results in Section V to show the performance of all adaptation models and conclude the paper in Section VI.

II. IR-HARQ MODELING

We consider a type-II HARQ system using RCPC code with single-transmit single-receive antenna in Fig. 1. The transmitter is equipped with a finite buffer that can accommodate B packets. Discrete-time representation of relevant variables is adopted in this paper. The discrete duration of transmission/retransmission, decoding of received packets and observation feedback constitutes a time-slot (also referred to as block). We represent the duration of each discrete time-slot with T_B . In general, the transmission/retransmission interval is smaller than the time-slot. However for simplicity of notation, unless otherwise specified, it will be assumed that transmission/retransmission interval is equal to T_B . Thus, time-slot k is the interval between time t^k and time t^{k+1} . Unless otherwise specified, we use superscript k to denote the value of particular variable at k^{th} time-slot. We assume the channel condition is known at the transmitter perfectly through noiseless feedback channel.

A. System Model

Let a^k denotes the number of incoming packets at the buffer in time-slot k . We assume that the incoming traffic is non-constant, and is independent and identically distributed (IID) with $P(a_i)$ being the probability of a_i packets arrival. In particular, for Poisson distributed traffic, the probability of a_i packet arrivals in time-slot k can be given by $P(a^k = a_i) = \exp(-\lambda T_B) \frac{(\lambda T_B)^{a_i}}{a_i!}$; $a_i \in \{0, 1, \dots, A\}$, where A is the maximum number of packet arrivals in a time-slot and $P(a^k = A) \rightarrow 0$. Therefore, the state space of the incoming traffic can be expressed as $\mathcal{A} = \{a_0, a_1, \dots, a_A\}$.

Assume that at the start of decision-epoch $n \in \mathbb{Z}^* = \{0, 1, \dots\}$, the scheduler chooses a particular action u^n to transmit w^n packets from the buffer. The buffer occupancy b^n and channel condition c^n in decision-epoch n determines the choice of action u^n . Each decision-epoch consists of 1 up to a maximum of $R + 1$ time-slots, where R is the maximum number of retransmissions. The duration of the decision-epoch is random variable and depends on the decoding result. The control action is taken at the start of a decision-epoch and the same action is continued until the end of that decision-epoch. Each control action corresponds to a specific modulation constellation and transmitter power level. We denote decision-epoch by superscript n to distinguish it from the time-slot.

Let $\mathcal{B} = \{b_0, b_1, \dots, b_B\}$ denotes the buffer state space in terms of packet occupancy, where b_i corresponds to $i \in \{0, 1, \dots, B\}$ packets in the buffer. Note that no transmission is possible when the buffer has insufficient number of packets for transmission. That is, the transmitter is in idle mode when

$b^{n+1} < \underline{w}$, where \underline{w} is the least number of packets that can be transmitted with any action. The buffer dynamic that gives the number of packets in the buffer at the start of a particular decision-epoch can be given by,

$$b^{n+1} = b^n - \eta w^n + a^k + \dots + a^{k+r} \quad (1)$$

where the multiplier η has value of 1 for positive acknowledgment (ACK) and 0 for negative acknowledgment (NAK) feedback in the last retransmission. In (1), $a^n = a^k$ is to be assumed and r is the random variable that characterizes the number of retransmission. Note that the ACK and NAK feedback from the receiver that reflect the decoding result constitute the observation for the IR-HARQ scheme.

Let $C_1 > C_2 > \dots > C_K$ denote the K rates offered by a family of RCPC codes which are obtained from a best low rate code $C_K = 1/N$ (e.g., 1/2 or 1/3). Parity check bits m_{crc} for error detection, and tail bits m_{tb} to properly terminate the encoder memory and decoder trellis are appended with $m_{ib} = w^n G$ information bits that correspond to w^n packets taken from the buffer, where G is the size of each incoming data packet in bits. Total $m_T = m_{ib} + m_{crc} + m_{tb}$ bits are encoded with the original mother code of rate C_K encoder. In the first transmission, code bits in the starting code C_1 are sent to the receiver over the correlated fading channel with the modulation constellation and transmitter power level determined by the scheduler. A Viterbi decoder is used for error correction followed by cyclic redundancy check (CRC) error detection. If no error is detected, the receiver sends an ACK to the transmitter and next decision-epoch starts; otherwise, the receiver sends a NAK. The incremental redundancy bits yielding code C_2 from code C_1 , which were deleted by puncturing process, are then transmitted and decoding is performed using code C_2 by combining the first and second sets of transmitted bits. This process is continued until decoding process results in no error being detected or the maximum number of retransmissions is reached. In either case, the buffer occupancy is updated and the whole process is started in next decision-epoch. Note that, the maximum number of retransmissions is less than the number of available rates K and the Viterbi decoding process is performed by combining the current and all the previous received bits to form a lower rate code for error correction.

B. Rayleigh Fading Finite State Markov Channel

The wireless channel in the analyzed IR-HARQ system is assumed to be ergodic flat fading obeying Rayleigh distribution. The probability density function of power gain for Rayleigh fading channel is described with exponential distribution [21],

$$f(\gamma) = \frac{1}{\bar{\gamma}} \exp\left(-\frac{\gamma}{\bar{\gamma}}\right), \text{ for } \gamma \geq 0, \quad (2)$$

where $\bar{\gamma} = \mathbb{E}\{\gamma\}$ is the average received channel power gain. We model the Rayleigh fading channel with a first order Markov model, which is described with a set of channel states $\mathcal{C} = \{c_1, c_2, \dots, c_C\}$ and a matrix of transition probabilities among states $\mathcal{P}_c = [P_{c_i, c_j}, 1 \leq i, j \leq C]$, where C is the number of finite non-overlapping channel states and P_{c_i, c_j}

is the probability of transition from state c_i to state c_j , i.e., $P_{c_i, c_j} = P(c_j | c_i)$, $1 \leq i, j \leq C$. The partitioning of the channel states can be done in several ways, e.g., in equal probability method, the stationary probability of all states are assumed to be equal. That is, $\phi_i = \int_{\gamma_{i-1}}^{\gamma_i} f(\gamma) d\gamma = 1/C, \forall c_i \in C$ [6]. Let $\Gamma = \{\gamma_0, \gamma_1, \dots, \gamma_C\}$ denotes the set of power gain threshold of the channel, where $\gamma_0 = 0$, $\gamma_i < \gamma_{i+1}$ and $\gamma_C = \infty$. The cross-over transition probabilities can be expressed in terms of Doppler frequency, f_m of the channel and block rate, R_B as,

$$P_{c_i, c_{i+1}} = \frac{N_i}{R_{B_i}}, \quad i = 1, 2, \dots, C-1 \quad (3)$$

and

$$P_{c_i, c_{i-1}} = \frac{N_{i-1}}{R_{B_i}}, \quad i = 2, 3, \dots, C, \quad (4)$$

where, $N_i = \sqrt{\frac{2\pi\gamma_i}{\gamma}} f_m \exp(-\frac{\gamma_i}{\gamma})$ is the level crossing rate at the threshold γ_i and $R_{B_i} = R_B \phi_i = \phi_i / T_B$ is average number of block per second in channel state c_i . Maximum Doppler frequency $f_m = v_{mt} / \lambda_{rw}$, where v_{mt} and λ_{rw} are the mobile station's speed and wavelength of the radio wave. When the fading rate of the channel is slow, the non-adjacent transition probabilities can be assumed to be zero, i.e., $P_{c_i, c_j} = 0$ if $|j - i| > 1$. Self transition probabilities can be found using the property that sum of all outgoing transition probabilities is equal to 1. In a special case when $C = 2$, the model can be described as Gilbert-Elliot channel containing a "bad" state (state c_1) and "good" state (state c_2). The steady-state probabilities of such two state channel can be given by $\phi_i = \frac{1 - P_{c_3-i, c_3-i}}{2 - (P_{c_1, c_1} + P_{c_2, c_2})}$, $i = 1, 2$.

C. RCPC Code and Observation Probability

In a family of rate compatible punctured convolutional codes, all the code-word bits of the higher-rate codes are embedded in the lower-rate codes, which guarantees smooth transition to different lower rates. A mother rate $1/N$ convolutional code is periodically punctured with period V to obtain a family of rate compatible convolutional code with decreasing rates, $\frac{V}{V+L}$, where L can be varied from 1 to $(N-1)V$. The operation of deleting bits from the output of the low-rate $1/N$ encoder is represented by a $N \times V$ puncturing matrix. A zero is used to indicate deleted bits. Therefore, for variable code-rate adaptive schemes, only the puncturing matrix needs to be chosen judiciously so that all the puncturing code of interest are obtained from the same low-rate encoder.

Assume that a code C_r is obtained from a family of RCPC codes by combining r successive transmissions starting with C_1 . Thus, given channel states $\{c^1, c^2, \dots, c^r\}$, the upper bound for the first error event probability of the Viterbi decoding algorithm with code C_r is expressed as [10],

$$P_E(C_r | c^1, c^2, \dots, c^r) \leq \sum_{d=d_{free}^{(r)}}^{\infty} \underbrace{\sum_{d^{(1)}} \sum_{d^{(2)}} \dots \sum_{d^{(r)}}}_{d^{(1)} + d^{(2)} + \dots + d^{(r)} = d} a_d^{(r)}(d^{(1)}, d^{(2)}, \dots, d^{(r)}) \times P_d(d^{(1)}, d^{(2)}, \dots, d^{(r)} | c^1, c^2, \dots, c^r), \quad (5)$$

where $d_{free}^{(r)}$ is the free distance of code C_r , and $a_d^{(r)}(d^{(1)}, d^{(2)}, \dots, d^{(r)})$ is the number of paths of weight d , $d^{(1)}$ is the distance contribution of code C_1 , $d^{(2)}$ is the contribution of the added bits to C_1 yielding code C_2 , and so on. The term $P_d(d^{(1)}, d^{(2)}, \dots, d^{(r)} | c^1, c^2, \dots, c^r)$ is the probability that a wrong path at distance d from the correct path is selected, given in eq. (12), [10] for hard-decision decoding. Our analysis also holds for soft-decision decoding under the assumption that fading changes slowly and is constant over duration of a decision epoch. The packet error rate for soft-decision decoding of convolutional codes, which is directly applicable to RCPC codes, can be found in [21] (Section 8-2-3, eq. (8-2-21)). It is understood that at the event of decoding success, i.e., when the received packets are totally error free, the transmitter received an ACK observation. Truncated ARQ, where the number of retransmissions are limited to finite number (e.g., 2 or 3), has been proven to increase throughput and decrease delay at the same time. However, successful transmission cannot be guaranteed even after R retransmissions and there is some probability of packet error [22].

Let us denote the event *{decoding failure with code C_r under channel states $\{c^1, c^2, \dots, c^r\}$ }* with *{NAK| c^1, c^2, \dots, c^r }*. The probability of *{NAK| c^1, c^2, \dots, c^r }* with action u is given by,

$$P_N(c^1, c^2, \dots, c^r, u) = 1 - (1 - P_E(C_r | c^1, c^2, \dots, c^r))^l, \quad (6)$$

where l is the number of stages in a trellis for decoding ($m_{ib} + m_{crc} + m_{tb}$) information bits with code $C_r = \frac{V}{V+L_r}$ and $l = \frac{m_{ib} + m_{crc} + m_{tb}}{V}$. Here, we assume that all the errors can be detected by the error detection code. The probability of the event *{decoding success with code C_r under channel states $\{c^1, c^2, \dots, c^r\}$ }*, i.e., the probability of *{ACK| c^1, c^2, \dots, c^r }* can be found as, $P_A(c^1, c^2, \dots, c^r, u) = 1 - P_N(c^1, c^2, \dots, c^r, u)$.

III. SMDP FORMULATION OF THE SCHEDULING PROBLEM FOR TYPE-II ARQ SYSTEMS

We have discussed in Section II that the time between successive control choices is variable and depends on the current state and the choice of action. The cost per decision-epoch depends on the time required for transition from one state to the next. Therefore, the problem at hand forms a semi-Markov decision process (SMDP) problem ([16], Section 5.3). The semi-Markov decision process problem can be modeled through a tuple $\{\mathcal{S}, \mathcal{U}, \mathcal{F}, \mathcal{Q}, \mathcal{G}\}$, where

- $\mathcal{S} = \{s_1, \dots, s_S\}$ is system state space that contains a finite number of states. The system state of the IR-HARQ problem at hand is composite and consists of buffer state and channel state. We represent it as $\mathcal{S} = \mathcal{B} \times \mathcal{C} = \{(b_0, c_1), (b_1, c_1), \dots, (b_B, c_C)\}$, where total number of states, $S = (B+1)C$.
- $\mathcal{U} = \{u_1, \dots, u_U\}$ is finite action space. We consider three adaptation models, where each action is mapped to a set of transmission parameters. The action mapping for these cases are discussed in Section III-A. We denote by $\mathcal{U}_s \subset \mathcal{U}$ those actions that are available at state $s \in \mathcal{S}$. The choice of action in a state is determined by a

policy. In general, the policy π in the policy space Π can be described as $\pi = \{\mu^1, \mu^2, \dots\}$, where action $u^n = \mu^n(s^n)$ is applied at decision-epoch n .

- Sojourn time for decision-epoch n , $T^n = t^{n+1} - t^n$ represents the time spent in a particular state before moving to the next state, where t^n is the time of occurrence of the start of the n^{th} decision-epoch with $t^0 = 0$ (see Fig. 1(b) for pictorial details). In IR-HARQ scheme, the sojourn time could be maximum 1 time-slot for first transmission, 2 time-slots for first retransmission, $R + 1$ time-slots for R retransmissions and depends on the channel state and the action chosen.
- \mathcal{Q} is the set of transition distributions (also called SMDP kernels) and $Q_{s_i, s_j}(\tau, u_i)$ represents the probability of moving from state s_i to state s_j at or before time τ if action u_i is chosen.
- \mathcal{G} is the set of cost matrices. We denote the cost associated with state-action pair (s, u) for objective “ X ” as $G^X(s, u)$. In this paper, we consider minimization of three objectives, namely, power, delay and buffer overflow. The costs associated with different objectives will be explained in Section III-C.

We consider the average cost criterion for scheduling packets in IR-HARQ schemes. There are two natural definitions of average cost per time-slot for SMDP. According to one definition, called time-average, the average cost is the limit of expected total costs for a specified policy π over the finite deterministic horizon divided by the length of the horizon,

$$G_t^\pi = \limsup_{T \rightarrow \infty} \frac{1}{T} \mathbb{E}_s^\pi \left\{ \int_0^T g(s(t), u(t)) dt \right\}. \quad (7)$$

According to the second definition, referred to as ratio-average, the average cost is the limit of the expected total costs over finite number of jumps divided by the expected cumulative time of these jumps,

$$G_r^\pi = \limsup_{m \rightarrow \infty} \frac{1}{\mathbb{E}_s^\pi \{T^m\}} \mathbb{E}_s^\pi \left\{ \int_0^{T^m} g(s(t), u(t)) dt \right\}, \quad (8)$$

where, $s(t) = s^n$ and $u(t) = u^n$ for $t^n \leq t < t^{n+1}$, and T^m is the completion time of the m^{th} transition. The expectation operator \mathbb{E}_s^π is the conditional expectation when the probability measure is determined by the policy π , and the conditioning event is $\{s^0 = s\}$. Although, in general these criteria are different, for the unichain problem at hand time-average cost equals ratio-average cost [16]. Therefore, we adopt second definition due to its analytical convenience.

A. Three Adaptation Models

We consider three different adaptation models for the IR-HARQ problem, each of which is described by choosing different set of transmission parameters of the SMDP problem. Let $\mathcal{E} = \{e_1, e_2, \dots, e_E\}$ denotes the set of all allowable transmitter power levels, and $\mathcal{W} = \{w_1, w_2, \dots, w_W\}$ denotes the set of available transmission rates that corresponds to the set of modulation constellations $\mathcal{V} = \{v_1, v_2, \dots, v_W\}$. Two mapping functions Φ and Ψ respectively map the action into the power level and transmission rate, i.e., $\Phi : \mathcal{U} \mapsto \mathcal{E}$ and $\Psi : \mathcal{U} \mapsto \mathcal{W}$.

1) *Power Adaptation with Constant Power throughout the Decision Epoch*: In this case, each action corresponds to a transmission power level and the number of transmission rates $W = 1$. The power level $P_t = \Phi(u^n)$ chosen at the start of a decision-epoch n is kept fixed until the end of that decision-epoch.

2) *Power Adaptation with Incremental Power for Additional Retransmission*: Changing transmission power level and taking corresponding action during the retransmission phase would be a more general problem, and may decrease the number of retransmissions compared to the case where control action is decided at the beginning of the decision-epoch and kept fixed during the retransmission phase as in Section III-A.1. However, this approach would considerably increase both the computational burden of the device and the memory needed for storing the optimal transmission policy. For example, if we consider the problem where transmitter power levels are adapted in each time-slot irrespective of new transmission or retransmission of an IR-HARQ system, the problem can be formed as a constrained Markov decision process, where the state space would have to be increased to include all the previous retransmission information. Therefore, to transmit a particular packets, all previous actions and channel states have to be tracked from the beginning of the new transmission up to the current retransmission. This is necessary to compute the probability of a packet error in a certain retransmission time-slot (see (5) for details) and form the costs to find the optimal policy. Storing previous action and channel states means that the state space would have to contain $B \times C \times (C \times U)^R$ states instead of $B \times C$ states when no transmission adaptation is considered during retransmission. This reduces the feasibility of the implementation of such policy even for moderate dimensionality of state and action space.

One way to deal with this problem is to use pre-decided increasing power levels in successive retransmission time-slots. We assume that the transmission rate throughout the decision-epoch remains the same, but transmission power is different in different time-slot. Let $e_i^{(t)}$ and $e_i^{(r)}$ denote the transmission power levels for first transmission and r^{th} retransmission respectively when an action corresponds to i^{th} power level has been chosen, i.e., $e_i = (e_i^{(t)}, e_i^{(1)}, \dots, e_i^{(r)})$. Therefore, each action corresponds to a set of power levels, where successive power levels are increasing and applied in consecutive retransmission time-slots.

3) *Joint Rate and Power Adaptation*: We adapt both the transmission rate and the power simultaneously for this model and therefore each action corresponds to a pair of transmission rate and power level. We denote the set of the pair of transmission rate and power by $\mathcal{X} = \mathcal{E} \times \mathcal{W} = \{x_1, x_2, \dots, x_U\} = \{(e_1, w_1), (e_1, w_2), \dots, (e_E, w_W)\}$.

B. SMDP Kernel and Transition Probability

The transition probability is defined as the probability of switching from current state to future state at/or before next decision-epoch. Therefore, for certain action, it determines the length of the decision-epoch in terms of time-slots. Since the transition probabilities and the costs for a state-action pair

depend on the length of the decision-epoch, the transition probability distribution is very important parameter for SMDP problems. Mathematically, transition distribution specifies the joint distribution of the transition interval τ and the next state s^{n+1} and for a given state-action pair (s^n, u^n) it can be expressed as [24]:

$$Q_{s^n, s^{n+1}}(\tau, u^n) = P\{t^{n+1} - t^n \leq \tau, s^{n+1} | s^n, u^n\}. \quad (9)$$

Let, for a particular fixed point T_f on the time-axis, $p(\tau, T_f)$ denotes a step function that has value 1 if $\tau > T_f$ and zero elsewhere. In practical systems, truncated HARQ with limited number of retransmissions have been found to optimize both the throughput and the delay, i.e., it increases the throughput and minimizes the packet delay in the buffer at the same time [11], [22]. It is also intuitively clear that rather than retransmitting large number of times, it is better to try limited number of times and if still decoding fails, then transmit again with higher transmission power and/or lower rate. Without loss of generality and to avoid cumbersome long expressions, we assume that the maximum number of retransmissions is two. Therefore, the transition distribution function can be expressed as,

$$\begin{aligned} Q_{s^n, s^{n+1}}(\tau, u^n) &= p(\tau, T_B)P_A(c^{n+1}|c^n, u^n)P_A(b^{n+1}|b^n, u^n) \\ &+ p(\tau, 2T_B)P_{N,A}(c^{n+1}|c^n, u^n)P_{N,A}(b^{n+1}|b^n, u^n) \\ &+ p(\tau, 3T_B)P_{N,N,A}(c^{n+1}|c^n, u^n)P_{N,N,A}(b^{n+1}|b^n, u^n) \\ &+ p(\tau, 3T_B)P_{N,N,N}(c^{n+1}|c^n, u^n)P_{N,N,N}(b^{n+1}|b^n, u^n) \end{aligned} \quad (10)$$

where, the channel transition probabilities upon getting observation for $c^{n+1} \in \mathcal{C}$ are given by,

$$P_A(c^{n+1}|c^n, u^n) = P_A(c^n, u^n)P_{c^n, c^{n+1}},$$

$$\begin{aligned} P_{N,A}(c^{n+1}|c^n, u^n) &= \sum_{c^{k+1}} P_N(c^n, u^n)P_A(c^n, c^{k+1}, u^n) \\ &\times P_{c^n, c^{k+1}}P_{c^{k+1}, c^{n+1}}, \end{aligned}$$

$$\begin{aligned} P_{N,N,A}(c^{n+1}|c^n, u^n) &= \sum_{c^{k+2}} \sum_{c^{k+1}} P_N(c^n, u^n) \\ &\times P_N(c^n, c^{k+1}, u^n)P_A(c^n, c^{k+1}, c^{k+2}, u^n) \\ &\times P_{c^n, c^{k+1}}P_{c^{k+1}, c^{k+2}}P_{c^{k+2}, c^{n+1}}, \end{aligned}$$

and

$$\begin{aligned} P_{N,N,N}(c^{n+1}|c^n, u^n) &= \sum_{c^{k+2}} \sum_{c^{k+1}} P_N(c^n, u^n) \\ &\times P_N(c^n, c^{k+1}, u^n)P_N(c^n, c^{k+1}, c^{k+2}, u^n) \\ &\times P_{c^n, c^{k+1}}P_{c^{k+1}, c^{k+2}}P_{c^{k+2}, c^{n+1}} \end{aligned}$$

The term $P_{N,N,A}(c^{n+1}|c^n, u^n)$, for example, is the probability of switching to channel state c^{n+1} from channel state c^n for action u^n , which causes NAK in the first transmission and in the first retransmission and causes ACK in the second retransmission. In (10), the term $P_{N,N,A}(b^{n+1}|b^n, u^n)$, for example, is the probability of occupying buffer state b^{n+1} from buffer state b^n for incoming traffic α^n and action u^n , which causes NAK in the first transmission and in the first

retransmission and causes ACK in the second retransmission and can be given by,

$$\begin{aligned} &P_{N,N,A}(b^{n+1}|b^n, u^n) \\ &= \sum_{\alpha^n \in \{0,1,\dots,3A\}} \delta\{b^{n+1} - (b^n - \Psi(u^n) + \alpha^n)\}P(\alpha^n), \end{aligned} \quad (11)$$

where $P(\alpha^n)$ is the probability of total $\alpha^n \in \{0, 1, \dots, l \times A\}$ packet arrivals in $l \in \{1, 2, 3\}$ time-slots, and $\delta(x)$ is a delta function whose value is 1 at $x = 0$ and zero otherwise. Other probability terms can be explained similarly. We assume that for all states s^n and s^{n+1} , and controls $u^n \in U_{s^n}$, $Q_{s^n, s^{n+1}}(\tau, u^n)$ are known and that the average transition time is finite, i.e., $\int_0^\infty \tau Q_{s^n, s^{n+1}}(d\tau, u^n) < \infty$. The expected value of the transition time corresponding to state-action pair (s^n, u^n) can be given by,

$$\begin{aligned} \bar{\tau}_{s^n}(u^n) &= \sum_{s^{n+1} \in \mathcal{S}} \int_0^\infty \tau Q_{s^n, s^{n+1}}(d\tau, u^n) \\ &= \sum_{c^{n+1}} T_B [P_A(c^{n+1}|c^n, u^n) + 2P_{N,A}(c^{n+1}|c^n, u^n) \\ &\quad + 3P_{N,N,A}(c^{n+1}|c^n, u^n) + 3P_{N,N,N}(c^{n+1}|c^n, u^n)]. \end{aligned} \quad (12)$$

As a consequence of choosing particular action u^n in a particular state s^n , the system moves to a new state s^{n+1} with probability given by transition probability. The transition probabilities can be specified by transition distributions via,

$$\begin{aligned} p_{s^n, s^{n+1}}(u^n) &= \lim_{\tau \rightarrow \infty} Q_{s^n, s^{n+1}}(\tau, u^n) \\ &= P_A(c^{n+1}|c^n, u^n)P_A(b^{n+1}|b^n, u^n) \\ &\quad + P_{N,A}(c^{n+1}|c^n, u^n)P_{N,A}(b^{n+1}|b^n, u^n) \\ &\quad + P_{N,N,A}(c^{n+1}|c^n, u^n)P_{N,N,A}(b^{n+1}|b^n, u^n) \\ &\quad + P_{N,N,N}(c^{n+1}|c^n, u^n)P_{N,N,N}(b^{n+1}|b^n, u^n). \end{aligned} \quad (13)$$

C. Costs Associated with Different Objectives

In this paper, our objective is to minimize three parameters that guarantee the QoS requirements for the IR-HARQ problem: transmitter power, buffer delay and packet overflow. We discuss the corresponding costs for achieving these objectives in the following sections. The one-stage expected transition cost for objective ‘‘X’’ corresponding to state-action pair (s^n, u^n) is defined as,

$$\begin{aligned} &G^X(s^n, u^n) \\ &= \sum_{s^{n+1}=s_1}^{s_S} \int_{\tau=0}^\infty g^X(s^n, u^n, s^{n+1}, \tau) \tau Q_{s^n, s^{n+1}}(d\tau, u^n). \end{aligned} \quad (14)$$

1) *Power Cost*: Minimizing transmission power is of particular importance for wireless devices that usually operate with battery of limited energy. The power cost for a particular state-action pair is the transmission power corresponding to that action and doesn't depend on future buffer state. The

immediate power cost for state-action pair (s^n, u^n) can be written as,

$$G^P(s^n, u^n) = \sum_{c^{n+1} \in \mathcal{C}} T_B [g^P(s^n, u^n, s^{n+1}, 1) P_A(c^{n+1} | c^n, u^n) + g^P(s^n, u^n, s^{n+1}, 2) P_{N,A}(c^{n+1} | c^n, u^n) + g^P(s^n, u^n, s^{n+1}, 3) P_{N,N,A}(c^{n+1} | c^n, u^n) + g^P(s^n, u^n, s^{n+1}, 3) P_{N,N,N}(c^{n+1} | c^n, u^n)], \quad (15)$$

where $g^P(s^n, u^n, s^{n+1}, 1) = e_i^{(t)}$ and $g^P(s^n, u^n, s^{n+1}, k) = e_i^{(t)} + e_i^{(1)} + \dots + e_i^{(k)}$, $k = 1, \dots, R$ are the immediate power cost for first transmission and total upto k^{th} retransmission respectively². For Section III-A.1 and Section III-A.3, the transmitter power doesn't change during the decision-epoch, therefore, $e_i^{(t)} = \dots = e_i^{(R)}$. It can be noted that (15) is sum of four terms. The first term is due to ACK in the first time-slot, the second term is due to NAK and ACK in the first and second time-slots respectively, the third term is due to NAK, NAK and ACK in the first, second and third time-slots respectively, and the fourth term is due to NAK, NAK and NAK in the first, second and third time-slots respectively.

2) *Buffer Delay Cost*: Since different traffic have different delay sensitivity, delay is another important parameter that quantifies QoS requirements in modern wireless networks. It can be noted that since packets are coming in each time-slot, delay is not fixed throughout the decision-epoch. The immediate delay cost, therefore, for IR-HARQ problem depends on the present buffer state as well as the next buffer state, and on the stochastic evolution of the buffer occupancy between two decision epochs. We proposed three variants of approximate immediate cost in this paper. We show their differences numerically in Section V. We take $g^D(s^n, u^n, s^{n+1}) = (b^n - 1)/\lambda$, $g^D(s^n, u^n, s^{n+1}) = (b^{n+1} - 1)/\lambda$ and $g^D(s^n, u^n, s^{n+1}) = 0.5(b^n + b^{n+1} - 2)/\lambda, \forall c^n, c^{n+1} \in \mathcal{C}$ as the immediate delay cost per time-slot for the three analyzed cases. For example, the third choice is based on the approximation that the buffer occupancy changes linearly between the successive decision-epochs. The expected delay cost for the IR-HARQ system with two retransmission is given by,

$$G^D(s^n, u^n) = \sum_{b^{n+1} \in \mathcal{B}} \sum_{c^{n+1} \in \mathcal{C}} g^D(s^n, u^n, s^{n+1}) \times T_B [P_A(c^{n+1} | c^n, u^n) P_A(b^{n+1} | b^n, u^n) + 2P_{N,A}(c^{n+1} | c^n, u^n) P_{N,A}(b^{n+1} | b^n, u^n) + 3P_{N,N,A}(c^{n+1} | c^n, u^n) P_{N,N,A}(b^{n+1} | b^n, u^n) + 3P_{N,N,N}(c^{n+1} | c^n, u^n) P_{N,N,N}(b^{n+1} | b^n, u^n)]. \quad (16)$$

3) *Buffer Overflow Cost*: It can be noted that while the scheduler is trying to send packets in a particular time-slot,

²The above power cost formulation can also account for unequal transmission intervals in different equal duration time-slotted retransmissions by weighting transmission power levels with appropriate factors. For example, for a maximum of two retransmission scheme, if the transmission interval of the first transmission is $\omega_1 T_B$ and transmission intervals of second and third retransmission are $\omega_2 T_B$ and $\omega_3 T_B$ respectively, then the transmission power levels should be weighted to $\omega_1 g^P(s^n, u^n, s^{n+1}, 1)$, $\omega_2 g^P(s^n, u^n, s^{n+1}, 2)$ and $\omega_3 g^P(s^n, u^n, s^{n+1}, 3)$

some incoming packets may be dropped due to insufficient space in the buffer. Therefore, packet overflow rate from the buffer is an important QoS requirements when the incoming traffic is bursty and the buffer is of finite length. The buffer overflow rate costs depend on the current buffer occupancy, maximum number of packets that can come in a time-slot and the observation for certain action and channel state. When the buffer has $B - A + 1$ or more packets, then $0, 1, 2, \dots$, up to a maximum of $3A$ packets can be dropped as a result of overflow. The expected overflow rate cost for above buffer states can be given by,

$$G^O(s^n, u^n) = \sum_{c^{n+1} \in \mathcal{C}} T_B [P_A(c^{n+1} | c^n, u^n) \sum_{\alpha^n = 1+r^n}^A P(\alpha^n)(\alpha^n - r^n) + P_{N,A}(c^{n+1} | c^n, u^n) \sum_{\alpha^n = 1+r^n}^{2A} P(\alpha^n)(\alpha^n - r^n) + P_{N,N,A}(c^{n+1} | c^n, u^n) \sum_{\alpha^n = 1+r^n}^{3A} P(\alpha^n)(\alpha^n - r^n) + P_{N,N,N}(c^{n+1} | c^n, u^n) \sum_{\alpha^n = 1+r^n}^{3A} P(\alpha^n)(\alpha^n - r^n + \Phi(u^n))], \quad (17)$$

where, r^n is maximum number of packets that can be accommodated without overflow and equals $B + \Phi(u^n) - b^n$. Note that when $B - 2A + 1 \leq b^n \leq B - A$, the number of packets that can be dropped due to overflow is $0, 1, 2, \dots$ up to a maximum of $2A$. Therefore, the expected overflow cost is given by the sum of last three terms of (17). When $B - 3A + 1 \leq b^n \leq B - 2A$, the number of packets that can be dropped due to overflow is $0, 1, 2, \dots$ up to a maximum of A . The expected overflow cost for these buffer occupancies can be given similarly. For all other buffer occupancies, no packet overflow occurs, therefore the cost is zero.

IV. SOLUTION TECHNIQUES

Semi-Markov average cost problem formulated in Section III can be transformed into an auxiliary discrete-time average cost problem, which can be solved easily with the dynamic programming algorithms for DT-MDP. The details of the equivalence between the SMDP and DT-MDP is discussed in Appendix I. We consider constrained Markov decision process (CMDP) formulation for the equivalent DT-MDP problem. The motivation of taking CMDP formulation is its mathematical artistry of solving problem with large number of states and easy incorporation of more than one constraints.

A. Constrained MDP Formulation

The CMDP problem can be expressed by the following equations, where our objective is to find optimal policy π^* over the set of all stationary policies Π that satisfy [24],

$$\min_{\pi \in \Pi} \tilde{G}^{P\pi}, \text{ subject to: } \tilde{G}^{D\pi} \leq D \text{ and } \tilde{G}^{O\pi} \leq P_{\text{of}}. \quad (18)$$

Long-term expected average power cost for policy π can be given by,

$$\tilde{G}^{P\pi} = \limsup_{m \rightarrow \infty} \frac{1}{m} \mathbb{E}_\pi \left[\sum_{n=1}^m \tilde{G}^{P\pi}(s^n, \pi(s^n)) \right]. \quad (19)$$

Constrained long-term expected costs $\tilde{G}^{D\pi}$ and $\tilde{G}^{O\pi}$ in (18) for policy π can be given similarly. Nonnegative constants D and P_{of} are the maximum allowable long-term average delay and long-term average overflow rate. The choice of these parameters depends on the QoS requirements of a particular application. The constraints (18) are called active if the equality holds for the optimal policy π^* . The CMDP formulation can be solved using linear programming method as given in Appendix II.

B. Effect of the Delay and Packet Overflow on Transmission Power

In this section, we analytically show that the optimal average power of the auxiliary DT-MDP problem is a non-increasing and convex function of the average buffer delay and the average packet overflow. Let $G^*(D, P_{of})$ denotes the average power needed by the optimal policy $\pi^*(s, u)$ to maintain certain feasible average delay D and feasible average overflow P_{of} . Thus, for fixed D and P_{of} , no other policy can achieve average power smaller than $G^*(D, P_{of})$. Therefore, $G^*(D, P_{of})$ also defines the lower bound on the achievable region of transmission powers for any policy. Theorem 1 provides the characterization of that region.

Theorem 1: For the adaptation problem defined in Section III, we can state the following: (1) achievable region of the average power $G^*(D, P_{of})$ is a non-increasing function of the average buffer delay D and the average packet overflow P_{of} , i.e., $G^*(D^2, P_{of}^2) \leq G^*(D^1, P_{of}^1)$ for some feasible constraints $D^2 \geq D^1$ and $P_{of}^2 \geq P_{of}^1$, and (2) $G^*(D, P_{of})$ is a jointly convex function of the average buffer delay D and the average packet overflow P_{of} . \circ

The proof of Theorem 1 is given in Appendix III.

V. SIMULATION RESULTS

In this section, we present simulation results, unless otherwise specified, for the following sets of data: number of channel states $C = 2$, buffer size $B = 100$ packets, average channel gain $\bar{\gamma} = 1$, noise power $\sigma^2 = 1$ mW, maximum number of retransmissions $R = 2$, block rate $R_B = 10^4$ blocks/sec, average arrival rate $\lambda = 1$ packet/time-slot, maximum number of packets arrival in a particular time-slot $A = 7$, number of actions $U = 3$ and binary phase shift keying (BPSK) transmission. The bit error rate (BER) expression for BPSK is given in [21], where the received signal to noise ratio is $P_r = \frac{\tilde{\gamma}_i P_t}{\sigma^2}$. The transmission power P_t may depend on the action taken and on the particular time-slot within a particular decision-epoch. The term $\tilde{\gamma}_i$ is the average channel gain of state c^i , which is computed using $\tilde{\gamma}_i = \frac{1}{\phi_i} \int_{\gamma_{i-1}}^{\gamma_i} \gamma f(\gamma) d\gamma$. The set of rates of the family of RCPC codes at the transmitter is $\{1, 1/2, 1/3\}$, which are generated from a parent rate $1/3$ code with memory $m_{tb} = 4$ (Table IV, [10]). We use LP to find optimal randomized scheduling policy and average transmission power for specified delay and overflow bounds.

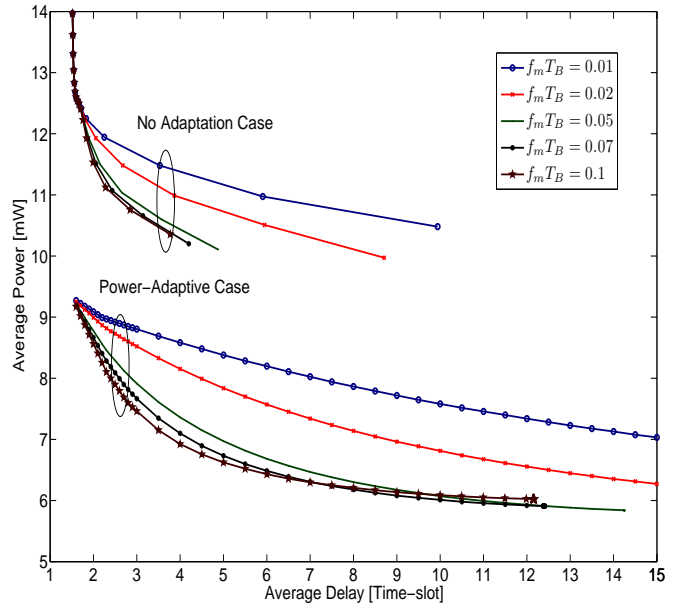


Fig. 2. Tradeoff between average transmitter power and average buffer delay for constant incoming traffic arrival, specified overflow bound and different fading rates. Comparison between power adaptive and no adaptation is shown.

Observation 1 (Power Adaptations Only): First we consider adaptation model given in Section III-A.1. We choose the set of power levels so that for all actions and channel states, the values of ACK/NAKs probabilities are distinct and provide diversity for the choice of power levels in different channel states. In Observation 3, we show an optimization procedure to calculate optimal power levels for specific delay and overflow constraint. For simulation purposes, we use the following: the set of power levels $\mathcal{E} = \{6.4, 15, 30\}$ mW, number of packets taken for transmission in each decision-epoch $w = 2$, and overflow bound $P_{of} = 10^{-4}$ for Figs. 2-7. When the scheduler has nothing to send, the transmit power is equal to zero as it is in idle state on that time. In Fig. 2, we show the tradeoff between the average transmission power and average buffer delay for constant incoming traffic of 1 packet/time-slot. It is seen from the figure that the power decreases as delay increases and the rate of decrease of power is more for faster fading channels in the lower delay regions. But in the higher delay regions, the rate of decrease of power is more for slower fading channels. For smaller delays, flexibility of storing packets is limited. Therefore, when the fading rate is slow, the scheduler has to choose higher transmission power to send the packets. For larger delays, the scheduler has more flexibility to store packets in bad channel states when the fading is slow and can allow more fluctuation in the buffer. Also, for slower fading the channel states in a decision-epoch are more predictable, therefore the decoding success is increased. Hence, in these regions the faster fading channels needs more power. We also compare the achievable average power vs. average delay curves for adaptive and non-adaptive cases. For non-adaptive case with specified bound of 10^{-4} on the average packet overflow, we vary the immediate transmission power from 30 mW to 7 mW, and find the average power and the average delay. It can be seen that

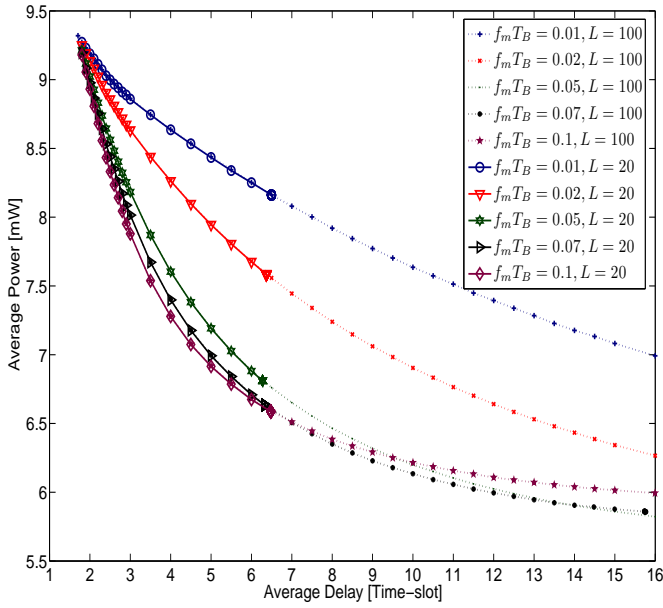


Fig. 3. Tradeoff between average transmitter power and average buffer delay for Poisson distributed incoming traffic arrival, specified overflow bound and different fading rates. The effect of different buffer sizes is also shown.

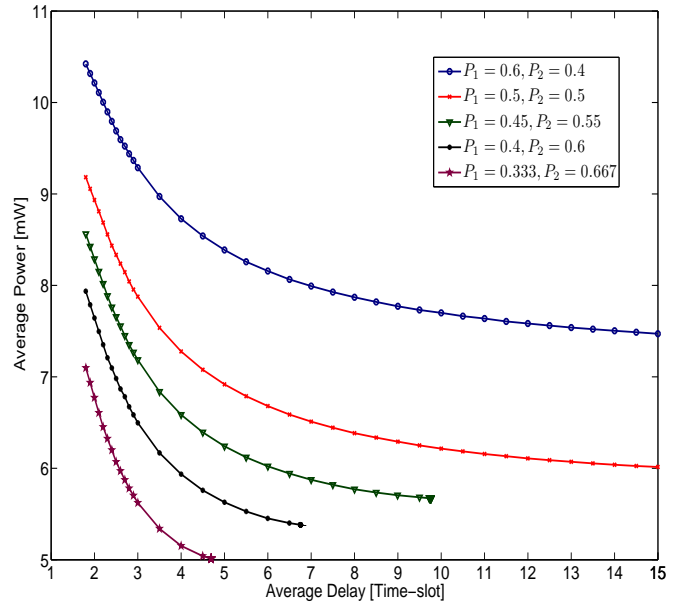


Fig. 5. The effect of unequal channel state stationary probability on the average transmitter power vs. average buffer delay curves for fixed number of channel states and packet overflow bound.

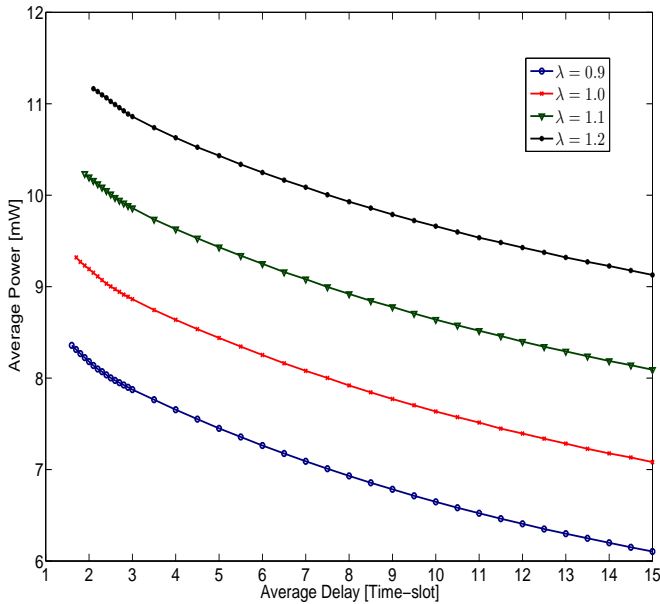


Fig. 4. The influence of different packet arrival rates on the average transmitter power/average buffer delay tradeoff for fixed buffer size and packet overflow bound.

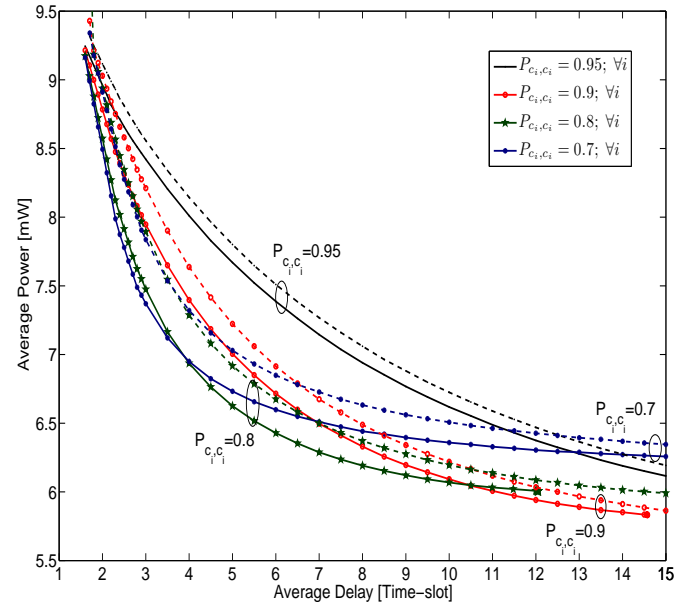


Fig. 6. Comparison of average transmitter power as a function of average buffer delay for constant (solid curves) and Poisson distributed (dotted curves) incoming packet arrival for different channel state memory and packet overflow bound.

the non-adaptive case needs approximately double average transmission power than the adaptive case for the same average delay and average overflow bounds.

Fig. 3 shows the effect of buffer sizes on the power/delay curves for different fading rates and same average rate Poisson distributed traffic. The figure shows the same trend as the constant traffic. Since the larger buffer gives more flexibility in terms of storing packet in lower channel state, the feasible delay region is larger and hence achievable average power is smaller.

The influence of different packet arrival rate with fixed buffer size is shown in Fig. 4. It is seen that for the same average delay, the average transmission power increases as average arrival rate increases. Since to maintain the same delay and overflow the scheduler has to send more packets with larger power in the lower channel state, the average transmission power increases as arrival rate increases.

The effect of unequal stationary probabilities of the channel states is shown in Fig. 5 for two states channel. The figure

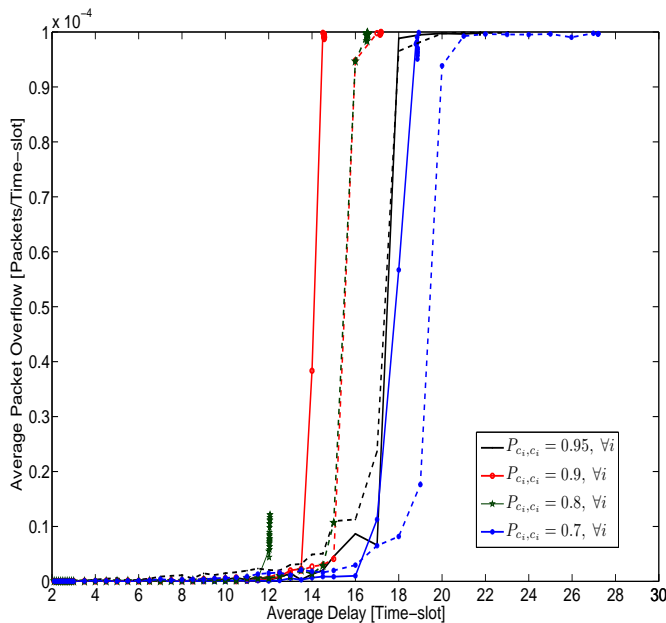


Fig. 7. Comparison of average packet overflow as a function of average buffer delay for constant (solid curves) and Poisson distributed (dotted curves) incoming packet arrival for different channel state memory and packet overflow bound.

shows that the average power increases as the stationary probability of lower channel state increases. Since the scheduler uses larger transmission power action to send packets in lower channel state, the average power increases with larger stationary probability of lower channel state due to longer stay there. In

Fig. 6, we give a comparison between the constant and Poisson distributed incoming traffic for the same average packet arrival rate of 1 packet/time-slot and different channel state memory. It is seen from the figure that the difference between transmission power for constant and Poisson traffic with same delay decreases as the fading correlation increases.

The packet overflows as a function of delay for constant and Poisson traffic is shown in Fig. 7. Note that to maintain fixed overflow rate, Poisson traffic suffers more delay. It can also be noticed that the packet overflow rate is almost zero in smaller delay region, but it increases as delay increases. Therefore, when the buffer size is large, overflow rate bound is not important in the lower delay regions. That is, in the lower delay regions, it is sufficient to fix a constraint on the average delay as the average overflow constraint does not represent an independent degree of freedom. But, in higher delay regions both are important to consider.

Observation 2 (FSMC-optimal policy in Jakes channel):

In order to evaluate the performance of the FSMC-optimal policy in realistic channels, we have simulated its performance in Jakes fading model for Rayleigh channel with both hard-decision and soft-decision decodings. In this observation, we analyze the performance of the optimal policy calculated for the FSMC channel model (such policy will be referred to as *FSMC-optimal policy*) when applied to the Jakes fading model with the same Doppler frequency. Since channel gains in Jakes model are not quantized, it cannot be directly modeled

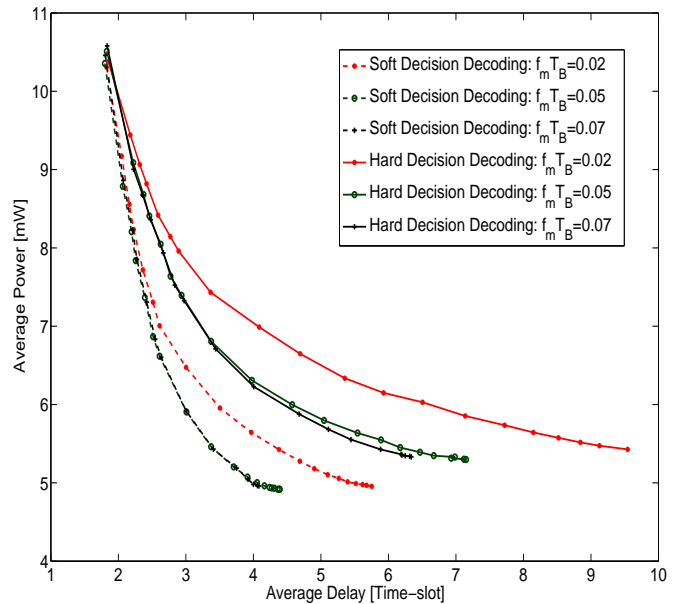


Fig. 8. Performance of the FSMC-optimal power scheduling policy in Jakes fading channel with Soft-decision and Hard-decision Decoding Schemes.

as a finite-state Markov channel. Therefore, to calculate the average power, delay and overflow costs, one has to calculate sample path average of these accrued costs over the ensemble of channel gain and incoming traffic realizations for a specific policy. The channel gain produced by the Jakes fading model is quantized with the threshold being the median value of the gain, as was done in the analytical calculation of the channel thresholds and transition probabilities of the two-state FSMC model. In Fig. 8, we show average power vs. average delay cost performance of the FSMC-optimal policies in Jakes fading channel for different fading rates. The FSMC-optimal policies are calculated for Poisson incoming traffic and for different delays using the same setting as the one shown in Fig. 3. Sample-path length of the simulation for the calculation of the average costs is taken to be 10000 slots. The traffic samples are generated using Poisson distributions and the number of paths in the Jakes model is 16. It can be easily noticed that average power-delay curve of the FSMC-optimal policies in Jakes fading channel follows the same general properties as in the FSMC channels. The average power also decreases with the increase of the delay as well as with the increase of Doppler frequencies for both the hard-decision and soft-decision decoding cases. However, as expected, for a particular delay, average power is less for soft-decision decoding than hard-decision decoding. The power saving facilitated by the use of soft-decision decoding compared with hard-decision decoding is increasing with the increase of the delay.

Observation 3 (Optimization of Power Levels): In this observation, we explain the choice of the power level set used in Observation 1. The optimal choice of power level set is made for a given constraint on average delay and a given constraint on average overflow. We carried out an outer nonlinear optimization to calculate the best power level set that gives minimum long-term average power for specific

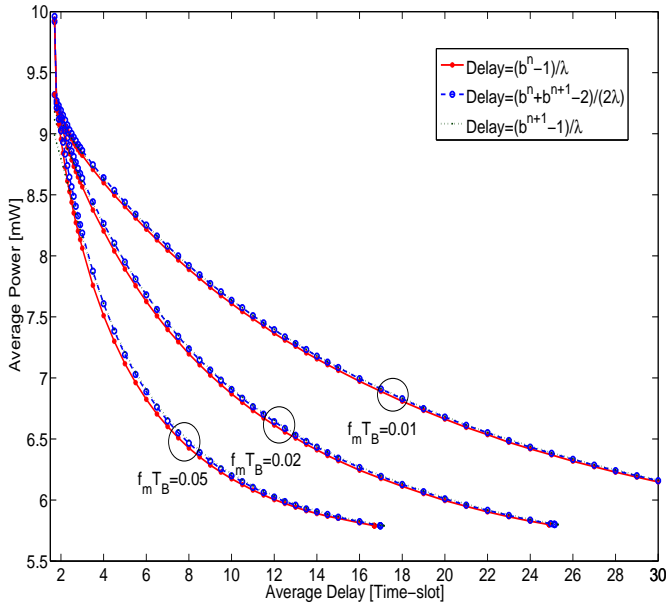


Fig. 9. Comparison of average power/average delay curves for different immediate delay cost models. All immediate delay cost models give approximately the same performance.

average delay and average overflow bounds. Therefore, the optimization problem is divided into two distinct problems: (1) inner dynamic programming optimization problem which provides the optimal power control law π^* and optimal average power $G^*(D, P_{of})$ for a fixed transmission power level set and (2) outer static optimization problem to choose the best set of transmission power levels that gives the minimum average power G_P^* . MATLAB optimization toolbox is used for this purpose. We computed optimal power level sets for average delay bounds from $D = 2$ to $D = 15$ and average overflow bound $P_{of} = 10^{-4}$. For example, the optimal power level set found for delay bounds $D = 4, 6, 10$ and 15 are respectively as follows: $\mathcal{E}^* = [6.8524 \ 14.9988 \ 29.9380]$ mW, $[6.8151 \ 14.9192 \ 29.6175]$ mW, $[6.5433 \ 15.5318 \ 29.6426]$ mW and $[6.4000 \ 15.1252 \ 23.8367]$ mW. The corresponding optimal average powers are 7.1769, 6.6073, 6.1859 and 6.0265 mW respectively. From the calculated optimal power level sets for different delays, we choose $[6.4 \ 15 \ 30]$ mW for our simulations. The optimal average power for this set and above delays are as follows: 7.2808, 6.6786, 6.2154 and 6.0351 mW respectively. The simulation results are given for $B = 50$ packets, $f_m T_B = 0.1$ and Poisson distributed traffic.

Observation 4 (Comparison between Different Buffer Costs): In Section III-C.2, we have proposed three approximations for the immediate costs that account for the delay in the transmission buffer. These three different immediate costs model the change of the buffer occupancy and delay between two subsequent decision-epochs in three different ways. In Fig. 9, we explore the influence of these models on the power vs. delay performance for the same set of data as Fig. 3. It can be seen that the choice of the immediate delay cost does not significantly influence the power performance of the IR-HARQ scheme. Therefore, whatever delay cost among these three costs in this framework is chosen, the results are

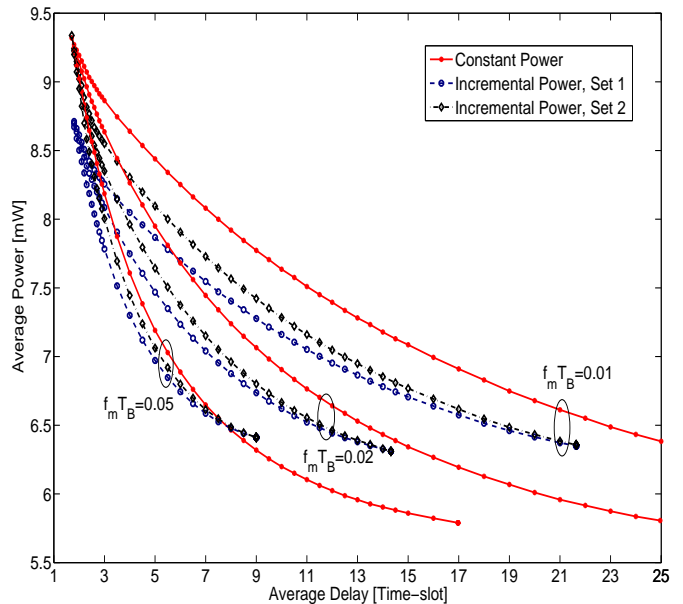


Fig. 10. Tradeoff between average transmitter power and average buffer delay for constant and incremental transmission power during a particular decision-epoch. For suitably chosen incremental power sets, incremental power actions outperform constant power actions.

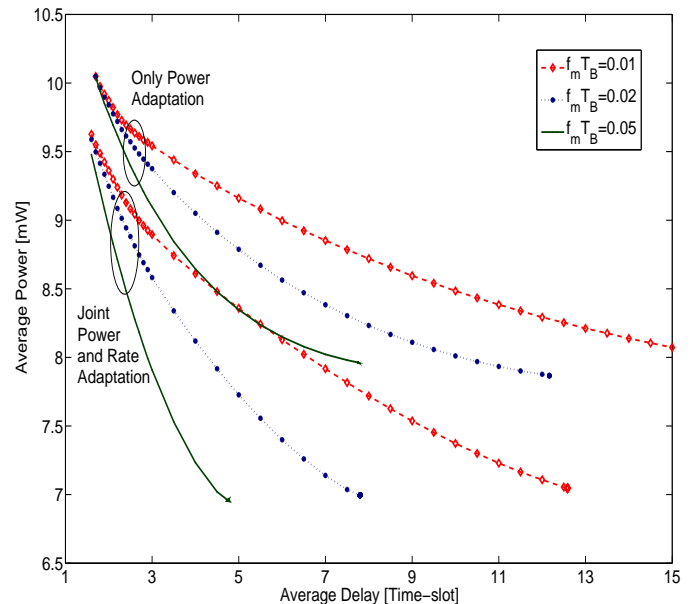


Fig. 11. Comparison of only power adaptation with combined rate and power adaptation. Joint power and rate adaptation provides better performance than only power adaptation due to the addition of more degrees of freedom in the action set.

the same.

Observation 5 (Incremental Power Adaptations): The performance of incremental power adaptation in successive time-slots is shown in Fig. 10 for Poisson traffic with $A = 7$. Two sets of transmission power are used to compare the performance with constant power described in Observation 1. Sets 1 and 2 are respectively as follows: $\mathcal{E} = \{(6.4, 8, 10), (15, 17, 20), (25, 27, 30)\}$ mW and $\mathcal{E} =$

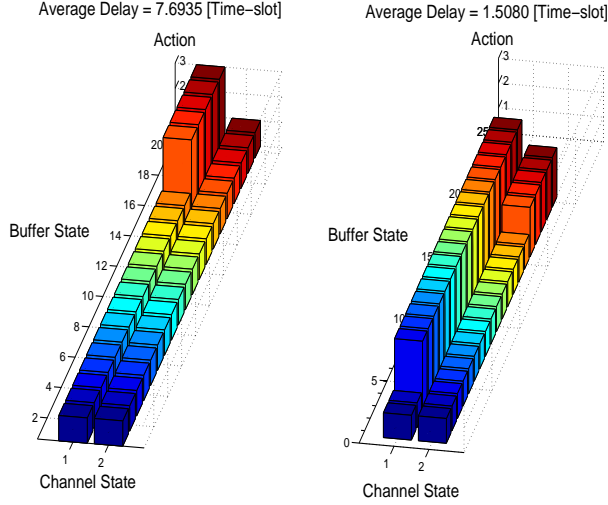


Fig. 12. Optimal policies are shown as a function of channel state and buffer state. For fixed sets of Lagrangian multipliers, we used relative value iteration (RVI) algorithm to compute optimal deterministic policies by solving corresponding Bellman's equation iteratively. We consider only power adaptation with constant traffic for this plot. In each subplot, the average overflow is below 10^{-4} .

$\{(6.4, 8, 10), (15, 18, 22), (30, 32, 35)\}$ mW. It is seen that the performance of the incremental power in general is better than constant power case. But, one need trials or outer optimization to find best set of incremental power. In our example, power set 1 performs better than set 2.

Observation 6 (Rate and Power Adaptations): Results for third adaptation model described in Section III-A.3 are given in Fig. 11 for Poisson traffic with $A = 7$ and $P_{of} = 10^{-4}$. The set of transmission parameters is $\mathcal{X} = \{(9.4, 2), (9.4, 3), (20, 2), (20, 3), (30, 2), (30, 3)\}$, where 4-QAM and 8-QAM are used to transmit 2 and 3 packets respectively. The approximate expression for BER of M-ary quadrature amplitude modulation (M-QAM) that is valid for both low and high SNR is derived in [23] (eq. (18)). The performance for joint rate and power adaptation is compared with only power adaptation case with 4-QAM and the same set of power levels $\mathcal{E} = \{9.4, 20, 30\}$ mW. It is revealed from the figure that as the joint rate and power adaptation has more degrees of freedom and hence wider range of action set, the power needed for the same delay is less compared to only power adaptation case.

Observation 7 (Policy Structure): Finally, in Fig. 12 we show the variation of the optimal policy with the current buffer and channel states. The optimal deterministic policies have been computed for two sets of Lagrangian multipliers. It can be seen that for larger average delays, the optimal scheduler applies less aggressive transmission policy. That is, it can delay applying action associated to larger powers until larger buffer occupancies.

VI. CONCLUSIONS

SMDP framework has been utilized to calculate the optimal rate and power adaptation policies of an IR-HARQ system. To the best knowledge of the authors, this is the first result that analyzes the rate and power adaptation under latency and overflow constraint for an IR-HARQ system designed to service a real-time traffic stream. For the stated IR-HARQ system with finite transmission buffer, we have derived the SMDP kernel, transition probability and costs associated with different objectives. The SMDP problem has been then converted into an auxiliary discrete-time CMDP problem and its solution is obtained by linear programming.

Simulation results have been given to examine the influence of randomly varying channel and traffic parameters for three different transmission models to allocate rate and power policy optimally. It has been shown that by employing optimal power allocation, fast fading channels perform the best under stringent delay constraints, while the situation is the opposite if delay constraints are relaxed. Simulation results show that FSMC-optimal scheduling policy performs very well in realistic channel (such as employing Jakes fading model for Rayleigh channel) and traffic settings. With the increased delay, soft-decision decoding gives more power savings compared to the hard-decision decoding. Significant power savings can be achieved with either incremental power allocation policy or joint rate and power allocation policy as compared to only power allocation policy.

APPENDIX I

EQUIVALENT AUXILIARY DISCRETE-TIME MDP FORMULATION FOR SMDP

Let us assume that $P_{s_i, s_i}(u_i) < 1$ for all $s_i \in \mathcal{S}$ and $u_i \in \mathcal{U}_{s_i}$, and γ be any scalar satisfying following inequality,

$$0 < \gamma < \frac{\bar{\tau}_{s_i}(u_i)}{1 - P_{s_i, s_i}(u_i)}. \quad (20)$$

The transition probability and the expected average cost per time-slot corresponding to state-action pair (s_i, u_i) for auxiliary discrete-time problem can be obtained respectively from,

$$\tilde{P}_{s_i, s_j}(u_i) = \begin{cases} \frac{\gamma P_{s_i, s_j}(u_i)}{\bar{\tau}_{s_i}(u_i)}, & \text{if } s_j \neq s_i, s_j \in \mathcal{S}; \\ 1 - \frac{\gamma(1 - P_{s_i, s_i}(u_i))}{\bar{\tau}_{s_i}(u_i)}, & \text{if } s_j = s_i, s_j \in \mathcal{S}. \end{cases} \quad (21)$$

$$\tilde{G}(s_i, u_i) = \frac{G(s_i, u_i)}{\bar{\tau}_{s_i}(u_i)} \quad (22)$$

A SMDP is considered *unichain* if every policy, μ^n induces a single recurrent class plus possibly an empty set of transient states (i.e., under every μ^n , the state process is an ergodic Markov chain). For finite SMDP with unichain structure and bounded costs, the optimal policy is stationary and Markovian, i.e., it is only dependent on the current system state. Note that the infinite horizon average cost of a finite unichain SMDP are not dependent on the initial state s^0 [24] and thus dependence on the initial state has been dropped from the notation. The analyzed transmission rate and power adaptation problem for the IR-HARQ system possesses the unichain structure. To prove this statement, we first note that the channel component of the state variable is independent on the actions

and its evolution is ergodic. Next, we demonstrate that the buffer component of the state variable is also ergodic under any policy. Let the current buffer state be b^n , then the next buffer state, b^{n+1} can fall into the interval of $[\max(b^n - w_1, 0), \dots, \min(b^n + (R+1)A, b_B)]$ with non-zero probability under any action. Repeating this reasoning for a sufficient number of decision-epochs, any buffer state is reachable from any other buffer state. Thus, the buffer state component of the state variable is also ergodic under any policy. This guarantees that the SMDP has a unichain structure.

The auxiliary DT-MDP and the SMDP have the same probabilistic structure [16]. Thus, if a stationary policy is unichain for SMDP problem, the same is true for the auxiliary DT-MDP problem. Therefore, dynamic programming (DP) algorithms for DT-MDP can be applied to the auxiliary problem in order to solve the semi-Markov problem. The multi-objective DT-MDP problem can be solved in two ways. In unconstrained Lagrangian formulation, the optimal policy is obtained iteratively using DP algorithm by solving the Bellman's optimality equation (cf. [25]). In constrained formulation, long-term average cost for one objective is minimized keeping other costs (called constraints costs) below some specified bounds.

APPENDIX II

LINEAR PROGRAMMING SOLUTION TECHNIQUE

Let $\nu(s, u)$ represents the "steady-state" probability that the process is in state s and action u is applied. We seek to find the control policy which is represented in terms of probability distribution ν over $\mathcal{S} \times \mathcal{U}$. The optimal policy ν^* can be obtained by solving the linear program:

$$\min_{\nu} \sum_{s_i \in \mathcal{S}, u_i \in \mathcal{U}_{s_i}} \tilde{G}^P(s_i, u_i) \nu(s_i, u_i) \quad (23)$$

subject to:

$$\sum_{s_i \in \mathcal{S}, u_i \in \mathcal{U}_{s_i}} \tilde{G}^D(s_i, u_i) \nu(s_i, u_i) \leq D$$

$$\sum_{s_i \in \mathcal{S}, u_i \in \mathcal{U}_{s_i}} \tilde{G}^O(s_i, u_i) \nu(s_i, u_i) \leq P_{\text{of}}$$

$$\sum_{u_i \in \mathcal{U}_{s_i}} \nu(s_j, u_i) = \sum_{s_i \in \mathcal{S}, u_i \in \mathcal{U}_{s_i}} \nu(s_i, u_i) P_{s_i, s_j}(u_i), \quad \forall s_j \in \mathcal{S}$$

$$\sum_{s_i \in \mathcal{S}, u_i \in \mathcal{U}_{s_i}} \nu(s_i, u_i) = 1; \quad \nu(s_i, u_i) \geq 0, \quad \forall s_i \in \mathcal{S}, \forall u_i \in \mathcal{U}_{s_i}.$$

Since there is an one-to-one correspondence between the feasible solution of the LP and the feasible solution of CMDP, then there exists an optimal randomized stationary policy μ^* for the CMDP problem if there exists an optimal solution ν^* to the LP problem [24]. The probability of applying action $u \in \mathcal{U}_s$ in state $s \in \mathcal{S}$ satisfies,

$$\theta_{\mu^*(s_i)}(u_i) = \frac{\nu^*(s_i, u_i)}{\sum_{u_j \in \mathcal{U}_{s_i}} \nu^*(s_i, u_j)} \text{ if } \sum_{u_j \in \mathcal{U}_{s_i}} \nu^*(s_i, u_j) > 0. \quad (24)$$

The linear program given above in (23) can easily and very efficiently be solved using interior point methods [26] or using optimization toolbox in any mathematical software package (e.g., function `linprog` in MATLAB).

APPENDIX III

PROOF FOR CONVEXITY PROPERTY

(1) The non-increasing property of function $G^*(D, P_{\text{of}})$ follows by noting the fact that increasing the constraints from (D^1, P_{of}^1) to (D^2, P_{of}^2) , the region of feasible policies defined in (18) is increased. Therefore, the global minimum achieved for the feasible region defined by constraints (D^1, P_{of}^1) is larger than or equal to the global minimum achieved for the feasible region defined by constraints (D^2, P_{of}^2) . That concludes the proof for the first part of the theorem.

(2) The convexity property of function $G^*(D, P_{\text{of}})$ can be established by a proof of contradiction. Suppose $G^*(D, P_{\text{of}})$ is a non-convex function of D and P_{of} , then there exist two pairs of feasible constraints (D_1, P_{of}^1) , (D_2, P_{of}^2) and a real number β in the range $0 < \beta < 1$ such that the inequality

$$\begin{aligned} & \beta G^*(D^1, P_{\text{of}}^1) + (1 - \beta) G^*(D^2, P_{\text{of}}^2) \\ & < G^*(\beta D^1 + (1 - \beta) D^2, \beta P_{\text{of}}^1 + (1 - \beta) P_{\text{of}}^2) \end{aligned} \quad (25)$$

holds. Let π_1^* , π_2^* and π_β^* be policies that are optimal for pair of constraints (D^1, P_{of}^1) , (D^2, P_{of}^2) and $(\beta D^1 + (1 - \beta) D^2, \beta P_{\text{of}}^1 + (1 - \beta) P_{\text{of}}^2)$ respectively. Due to ergodicity of the incurred Markov chain implied by the unichain structure, mixed policy π_β of policies π_1^* , π_2^* (where π_1^* and π_2^* are applied with probabilities β and $(1 - \beta)$ respectively for sufficient number of successive decision-epochs) attains the cost $\beta G^*(D^1, P_{\text{of}}^1) + (1 - \beta) G^*(D^2, P_{\text{of}}^2)$. Such mixed policy has larger or equal cost than the optimal cost of the minimization problem for the pair of constraints $(\beta D^1 + (1 - \beta) D^2, \beta P_{\text{of}}^1 + (1 - \beta) P_{\text{of}}^2)$. This is a contradiction to (25) and our initial assumption that $G^*(D, P_{\text{of}})$ is a non-convex function of (D, P_{of}) fails. Therefore $G^*(D, P_{\text{of}})$ is a jointly convex function of D and P_{of} .

REFERENCES

- [1] D. Garg and F. Adachi, "Packet access using DS-CDMA with frequency-domain equalization," *IEEE J. Select. Areas Commun.*, vol. 24, pp. 161-170, Jan. 2006.
- [2] R. Love, B. Classon, A. Ghosh, and M. Cudak, "Incremental redundancy for evolutions of 3G CDMA systems," in *Proc. of IEEE VTC'02*, vol. 1, pp. 454-458, 6-9 May 2002.
- [3] J. Hagenauer, "Rate-compatible punctured convolutional codes (RCPC) and their applications," *IEEE Trans. Commun.*, vol. 36, pp. 389-400, Apr. 1988.
- [4] D. Haccoun and G. B egin, "High-rate punctured convolutional codes for Viterbi and sequential decoding," *IEEE Trans. Commun.*, vol. 37, pp. 1113-1125, Nov. 1989.
- [5] Y. Jungnam and M. Kavehrad, "Markov error structure for throughput analysis of adaptive modulation systems combined with ARQ over correlated fading channels," *IEEE Trans. Veh. Technol.*, vol. 54, pp. 235-245, Jan. 2005.
- [6] H. S. Wang and N. Moayeri, "Finite-state Markov channel- a useful model for radio communication channels," *IEEE Trans. Veh. Technol.*, vol. 44, No. 1, pp. 163-171, Feb. 1995.
- [7] E. N. Gilbert, "Capacity of a burst-noise channels," *Bell Syst. Tech. J.*, vol. 39, pp. 1253-1266, Sep. 1960.
- [8] E. O. Elliott, "Estimates of error rates for codes on burst-noise channels," *Bell Syst. Tech. J.*, vol. 42, pp. 1977-1997, Sep. 1963.
- [9] S. Kallel and D. Haccoun, "Generalized type II hybrid ARQ scheme using punctured convolutional coding," *IEEE Trans. Commun.*, vol. 38, pp. 1938-1946, Nov. 1990.
- [10] Qinqing Zhang and S. A. Kassam, "Hybrid ARQ with selective combining for fading channels," *IEEE J. Select. Areas Commun.*, vol. 17, pp. 867-880, May 1999.

- [11] L. Lugand, D. J. Costello, Jr., and R. H. Deng, "Parity retransmission hybrid ARQ using rate 1/2 convolutional codes on a nonstationary channel," *IEEE Trans. Commun.*, vol. 37, pp. 755-765, Jul. 1989.
- [12] L. Lin, R. D. Yates, and P. Spasojević, "Adaptive transmission with discrete code rates and power levels," *IEEE Trans. Commun.*, vol. 51, pp. 2115-2125, Dec. 2003.
- [13] T. Ji and W. Stark, "Rate-adaptive transmission over correlated fading channels," *IEEE Trans. Commun.*, vol. 53, pp. 1663-1670, Oct. 2005.
- [14] A. K. Karmokar and V. K. Bhargava, "Coding rate adaptation for hybrid ARQ systems over time varying fading channels with partially observable state", in *Proc. of ICC'05*, May. 16-20, 2005, vol. 4, pp. 2797-2801.
- [15] D. Rajan, A. Sabharwal, and B. Aazhang, "Delay-bounded packet scheduling of bursty traffic over wireless channels," *IEEE Trans. Inform. Theory*, vol. 50, pp. 125-144, Jan. 2004.
- [16] D. P. Bertsekas, *Dynamic Programming and Optimal Control*, Second Edition, vol. II. Belmont, Massachusetts: Athena Scientific, 2001.
- [17] Wen-Bin Yang and E. Geraniotis, "Admission policies for integrated voice and data traffic in CDMA packet radio networks," *IEEE J. Select. Areas Commun.*, vol. 12, pp. 654-664, May 1994.
- [18] V. W. S. Wong, M. E. Lewis, and V. C. M. Leung, "Stochastic control of path optimization for inter-switch handoffs in wireless ATM networks," *IEEE/ACM Trans. Networking*, vol. 9, pp. 336-350, Jun. 2001.
- [19] C. Comaniciu and H. V. Poor, "Jointly optimal power and admission control for delay sensitive traffic in CDMA networks with LMMSE receivers," *IEEE Trans. Signal Processing*, vol. 51, pp. 2031-2042, Aug. 2003.
- [20] "cdma2000 High Rate Packet Data Air Interface Specification," *3RD Generation Partnership Project 2 (3GPP2) C.S0024-A*, version 3.0, Sep. 2006. [Online]. Available: http://www.3gpp2.org/Public_html/specs/C.S0024-A_v3.0_060912.pdf.
- [21] J. G. Proakis, *Digital Communications*. 3rd ed., New York: McGraw Hill, 2000.
- [22] E. Malkamäki and H. Leib, "Performance of Truncated Type-II Hybrid ARQ Schemes with Noisy Feedback over Block Fading Channels," *IEEE Trans. Commun.*, vol. 48, pp. 1477-1487, Sep. 2000.
- [23] Jianhua Lu, K. B. Letaief, J. C.-I. Chuang, and M. L. Liou, "M-PSK and M-QAM BER computation using signal-space concepts," *IEEE Trans. Commun.*, vol. 47, Feb. 1999, pp. 181-184.
- [24] M. L. Puterman, *Markov Decision Processes: Discrete Stochastic Dynamic Programming*. New York: John Wiley & Sons, 1994.
- [25] A. K. Karmokar, D. V. Djonin, and V. K. Bhargava, "Optimal and suboptimal packet scheduling over time-varying flat fading channels", *IEEE Trans. Wireless Commun.*, vol. 5, no. 2, pp. 446-457, Feb. 2006.
- [26] S. Boyd and L. Vandenberghe, *Convex Optimization*. UK: Cambridge University Press, 2004.



Ashok K. Karmokar (S'04) received the Ph. D. degree in Electrical and Computer Engineering from the University of British Columbia (UBC) in 2007. He received the B.Sc. and M.Sc. degrees in Electrical and Electronic Engineering from Bangladesh University of Engineering and Technology (BUET), Dhaka, Bangladesh in 1998 and 2002 respectively.

Currently, he is a Postdoctoral Fellow in the Department of Electrical and Computer Engineering at the University of British Columbia, Vancouver, Canada. From 1998 to 2002, he was with Bangladesh University of Engineering and Technology, where he served as a Lecturer and then as an Assistant Professor in the Department of Electrical and Electronic Engineering.

Dr. Karmokar is the recipient of Patrick David Campbell Graduate Fellowship, Ann and William Messenger Graduate Fellowship, University Graduate Fellowship, and Ph. D. Tuition Fee Award from the University of British Columbia. He is also the recipient of Excellence Recruitment Award from the University of Victoria, Dean's List Award, University Merit Scholarship, Altaf Hossain Fellowship and Dr. Rashid Memorial Scholarship from BUET, and Werner Von Siemens Excellence Award from Siemens AG.

His current research interests include cross-layer adaptive transmissions, resource allocations and packet scheduling for wireless broadband networks, sensor networks and cognitive radio networks.



Dejan V. Djonin received the B.Sc. and M.Sc. degrees from the University of Belgrade, Belgrade, Serbia, in 1996 and 1999, respectively, and the Ph.D. degree from the University of Victoria, Victoria, BC, Canada, in 2003.

From 1998 to 2000, he was with the Department of Telecommunications, Institute Mihajlo Pupin, Belgrade, where he worked on the development of an antenna-array signal processing system. He held NSERC Postdoctoral Fellowship at the Department of Electrical and Computer Engineering, the University of British Columbia, Vancouver, BC, Canada, in 2005 and 2006. Currently, he is with the Dyaptive Systems, Vancouver, BC, Canada, developing testing equipment for the 1xEV-DO and LTE base stations. Since February 2007, he has been Adjunct Professor at the Department of Electrical and Computer Engineering, University of British Columbia. His research interests include applications of control theory in multimedia wireless communication systems and sensor networks.

Dr. Djonin served as an Assistant Program Chair of the Wireless Communications and Networking Conference (WCNC) 2004 and as a Technical Program Committee Member of International Conference on Communications (ICC) 2005 and the IEEE GLOBECOM 2003 Conferences. In 2002, he was awarded the Outstanding Paper Award for Young Researchers at the International Symposium on Information Theory and its Application (ISITA) Conference.



Vijay K. Bhargava (S'70-M'74-SM'82-F'92) received the B.Sc., M.Sc., and Ph.D. degrees from Queen's University, Kingston, ON, Canada in 1970, 1972 and 1974 respectively.

Currently, he is a Professor and Head of the Department of Electrical and Computer Engineering at the University of British Columbia, Vancouver, Canada. Previously he was with the University of Victoria (1984-2003) and with Concordia University in Montreal (1976-1984). He is a co-author of the book *Digital Communications by Satellite* (New

York: Wiley, 1981), co-editor of *Reed-Solomon Codes and Their Applications* (New York: IEEE, 1994), co-editor of *Communications, Information and Network Security* (Boston: Kluwer, 2003) and co-editor of *Cognitive Wireless Communication Networks* (New York: Springer, 2007). His research interests are in wireless communications.

Dr. Bhargava is a Fellow of the Engineering Institute of Canada (EIC), the IEEE, the Canadian Academy of Engineering and the Royal Society of Canada. He is a recipient of the IEEE Centennial Medal (1984), IEEE Canada's McNaughton Gold Medal (1995), the IEEE Haraden Pratt Award (1999), the IEEE Third Millennium Medal (2000), IEEE Graduate Teaching Award (2002), and the Eadie Medal of the Royal Society of Canada (2004).

Dr. Bhargava is very active in the IEEE and was nominated by the IEEE Board of Directors for the Office of IEEE President-Elect. He has served on the Board of the IEEE Information Theory Society and the IEEE Communications Society. He is a Past President of the IEEE Information Theory Society. He is Editor-in-Chief of the *IEEE Transactions on Wireless Communications*.